Supporting Information

Phase Transformation of Sn-based Nanowires under Electron Beam Irradiation

Hong Zhang, ‡[a] Xia Deng, ‡[a] Junwei Zhang,[a] Desheng Xue,[a] Yuanqing Huang,[a] Feiming Bai,[b] Beverly. J. Inkson[c] and Yong Peng*[a]

Miss. H. Zhang, Miss. X. Deng, Mr. J. W. Zhang, Mr. Y. Q. Huang, Prof. D. S. Xue, Prof. Y. Peng
Key Laboratory of Magnetism and Magnetic Materials of Ministry of Education
Lanzhou University
Lanzhou 730000, Gansu (P. R. China)
E-mail: pengy@lzu.edu.cn

Prof. F. M. Bai
State Key Laboratory of Electronic Thin Films and Integrated Devices
University of Electronic Science and Technology
Chengdu 610054, Sichuan (P. R. China)

Prof. B. J. Inkson
Department of Materials Science and Engineering
University of Sheffield
Sheffield S1 3JD, UK

1. Chemical analysis of the $Sn_{78}Ag_{22}$ nanowires before thermal oxidation.

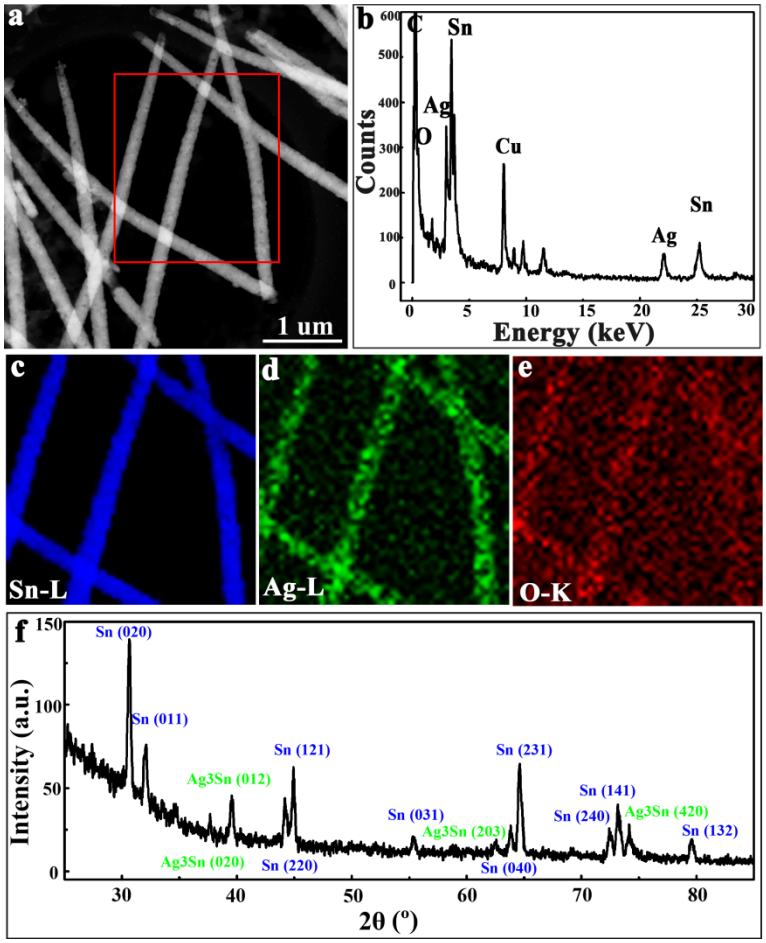

Figure S1. Chemical analysis of the Sn-Ag nanowires before thermal oxidation. **(a)** HAADF–STEM image of the fresh prepared Sn-Ag nanowires. **(b)** EDX spectrum acquired from nanowires marked by red square, referring a $Sn_{78}Ag_{22}$ chemical composition. (**c-e)** EDX elemental mappings of O-K, Ag-L and Sn-L acquired from nanowires marked by red square. **(f)** XRD patterns of the fresh prepared Sn-Ag nanowires embedded in template.

Figure S1a shows a representative HAADF–STEM image of the fresh prepared Sn-Ag nanowires. Their surfaces are smooth and do not show obvious defects, revealing a good qualify. Figure S1b shows the EDX spectrum acquired from

nanowires marked by red square in Fig. S1a. Quantitative analysis of EDX spectrum reveals that the chemical composition of the SnAg nanowires is a 78:22 weight ratio of Sn:Ag, referring a $Sn_{78}Ag_{22}$ chemical composition. Figure S1c-2e further show the EDX elemental mappings of Sn-Lα (3.44 keV), Ag-Lα (2.98 keV) and O-Kα (0.52 keV), respectively. The elements of Sn and Ag are almost evenly distributed throughout the whole nanowires, indicating a uniform $Sn_{78}Ag_{22}$ chemical phase. The smaller amounts of oxygen element reveals that individual $Sn_{78}Ag_{22}$ nanowires have been slightly oxidized after released from the template. Figure S1f shows a representative XRD patterns of the fresh prepared Sn-Ag nanowires embedded in template. Tetragonal β-Sn and orthorhombic Ag_3Sn can be matched in the patterns, indicating the successful alloying of Sn and Ag during the synthesis process. This was further confirmed through their crystal structures by HRTEM and CBED.

2. Structural analysis of the outside oxide layer of the $Sn_{78}Ag_{22}$ nanowires.

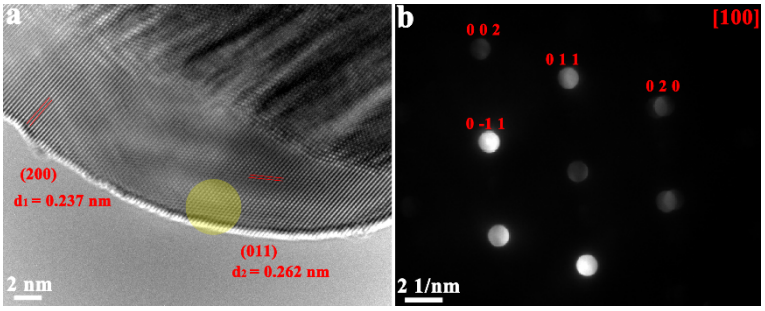

Figure S2. Structural analysis of the oxide layer of the $Sn_{78}Ag_{22}$ nanowires. **(a)** High-resolution TEM image of an investigated $Sn_{78}Ag_{22}$ nanowire after thermal oxidation treatment, of which contrast clealy reveals a stratified structure. **(b)** CBED pattern acquired from the nanowire marked by yellow circle in Figure S2a.

It is seen that a 4~10 nm thickness layer is covered on the surface of the $Sn_{78}Ag_{22}$ nanowire in Fig. 1 and Fig. S2, which is due to the oxidization. The crystal structure of the oxide layer was characterized in detail using high-resolution TEM (HRTEM) and convergent beam electron diffraction (CBED). Figure S2 shows a lattice-resolution image of an investigated $Sn_{78}Ag_{22}$ nanowire after thermal oxidation treatment. The interplanar distances are measured to be 2.37 Å and 2.62 Å, matching with (200) and (011) planes of tetragonal SnO_2. To further verify the accuracy of the crystal measurements, CBED using a 4 nm spot marked by yellow circle is used to analyze this area, which can be well indexed into [100] crystallographic orientation of tetragonal structure. This result is well matched with the HRTEM observation. It is then concluded that the stratified layer coved on the surface of $Sn_{78}Ag_{22}$ nanowire after thermal oxidation treatment is SnO_2, which has a similar crystal phase with that of Sn-3.5Ag nanowires.

3. EDX spectrum and EDX linescan spectra of $Sn_{78}Ag_{22}$ nanowires in Figure 3

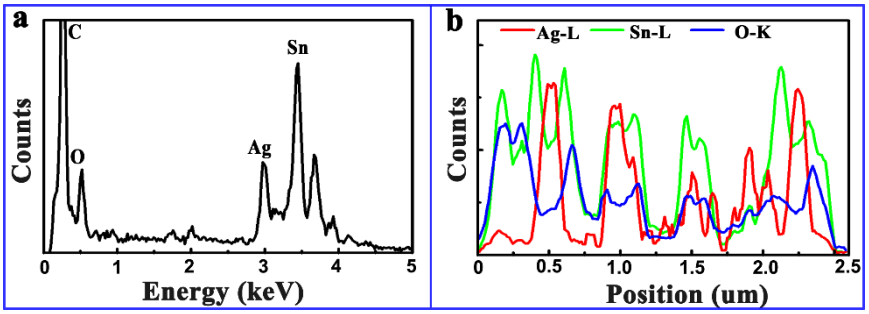

Figure S3. **(a)** EDX spectrum acquired from nanowire marked by red square in Figure 3a, referring a $Sn_{80}Ag_{20}$ chemical composition. **(b)** EDX line-scan spectra of

Sn-L, Ag-L and O-K taken across the nanowire 1 in Figure 3a, acquired using a 2.5 μm scan line parallel to the nanowire 1 axis as marked by blue line and a 1.5 nm beam spot-size.

4. Steering the phase transformation behavior of Sn-Pb alloy nanowires

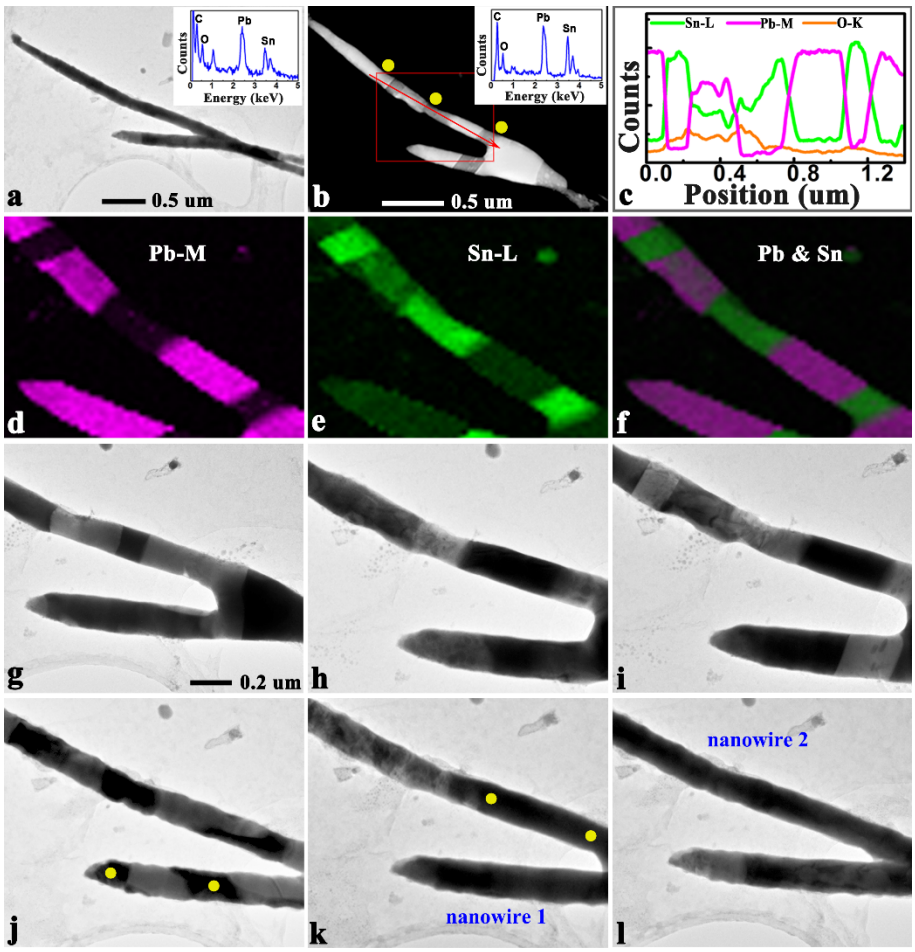

Figure S4. Phase transformation engineering of SnPb alloy nanowires under EBI. **(a)** A representative BF-TEM image of two SnPb nanowires, of which a thin oxide layer was intended to oxidize onto their surfaces. Inset, EDX spectrum before EBI treatment, referring a $Sn_{84}Pb_{16}$ chemical composition. (**b)** HAADF-STEM image after EBI, showing that the two nanowires have been sculpted into a multilayered nanostructure. Inset, EDX spectrum acquied from the red rectangle, referring a

$Sn_{80}Pb_{20}$ chemical composition. (**c)** EDX line-scan spectra of Sn-L, Pb-M and O-K from the nanowire marked by red line in Fig. S4b. (**d-f)** The corresponding EDX elemental mappings of Fig. S4b. (**g-i)** Sculpting of ordered nano-patterns via the selective e-beam irradiation. The yellow circles indicate the position of the e-beam spot. **(j-l)** selective EBI technique is used to precisely control the phase reversibility of the SnPb nanowires between precipitated phases and homogeneous alloy at the nanoscale, where (k) shows that nanowire 1 has been restored into its original homogeneous phase and (l) nanowire 2 has been restored into its original homogeneous phase.

Following the same mechanism, individual Sn-Pb alloy nanowires also can be steered to regulate phase aggregate states under e-beam irradiation. Figure S4 shows the morphological evolution and chemical distributions of the Sn-Pb alloy nanowires under e-beam irradiation. Figure S4a-S4f demonstrate that the Sn-Pb alloy nanowires with an oxide layer outside can also appear concentrational stratification. Figure S4a shows a representative BF-TEM image of two Sn-Pb nanowires, of which a thin oxide layer was covered on their surface for providing a pip-like spatial confinement. The nanowires were firstly irradiated by a spread e-beam until the inner alloy became fluid, which flowed in the nano-pipe of SnO_2 oxide. A convergent e-beam was then placed in the regions pointed by the yellow circles successively to determine the size of phase-separation sections. After this procedure, nanowires were sculpted into concentrational stratification structure as showed in Figure S4b. Quantitative analysis

of EDS spectra before and after the irradiation (inset of Figure S4a and S4b) reveal that the chemical composition of the Sn-Pb nanowires has changed from $Sn_{16}Pb_{84}$ to $Sn_{20}Pb_{80}$. Figure S4c shows EDX line-scan spectra of Sn-Lα, Pb-Mα and O-Kα taken along the red line in Figure S4b. It is seen that the intensities of Sn and Pb are inversely proportional. Figure S4d-f further show the EDX elemental mappings of Sn-Lα, Pb-Mα and the combination of Sn and Pb, respectively. It is seen that the elements of Sn and Pb appear aggregation, respectively. Figure S4 g-i show three different phase aggregation statuses by site-selective irradiation. The EBI technique also realizes a fusion of the precipitated phases, and their size- and position- changes at the nanoscale, which proves that the shapes and positions of the precipitated phases can be precisely steered. Thus, a controllable phase manipulation strategy of Sn-Pb alloy nanowires with an oxide layer outside under EBI has been demonstrated.

Figure S4j-l show how the selective EBI technique is used to precisely control the phase reversibility of the $Sn_{16}Pb_{84}$ nanowires between precipitated phases and homogeneous alloy at the nanoscale. By scanning the electron beam between the two yellow points in Fig. S4j back and forth several times, the nanowire 1 as shown in Fig. S4k has been restored into its original homogeneous phase. When the beam was scanned between the two yellow points in Fig. S4k, nanowire 2 has also been successfully restored original homogeneous phase. This result proves that the phase-change behavior of phase-change materials under electron beam irradiation phase is universal for Sn-based PCMs.